CRYSTAL GROWTH & DESIGN
2009
VOL. 9, NO. 7
3124–3128

Engineering Crystal Packing and Internal Dynamics in Molecular Gyroscopes by Refining their Components. Fast Exchange of a Phenylene Rotator by ^{2}H NMR

Miguel A. Garcia-Garibay* and Carlos E. Godinez

Department of Chemistry and Biochemistry, University of California, Los Angeles, California 90096-1569

Received September 22, 2008; Revised Manuscript Received April 13, 2009

ABSTRACT: Using quadrupolar echo ^{2}H NMR, we have determined that a relatively simple change on the periphery of the triptycene stators of molecular gyroscopes may have a profound effect on the packing arrangements, packing coefficients, and rotary dynamics of the central phenylene rotators. The previously reported crystal structure of 1,4-bis-[2-(9-triptycyl)-ethynyl]benzene (**1**) is characterized by the inclusion of *meta*-xylene and a very tightly interdigitated packing arrangement that effectively prevents the rotary motion of the phenylene rotator. Structural modifications to prevent this interdigitation led to the design and synthesis of 1,4-bis[2-(2,3,6,7,12,13-hexamethyl-10-propyl-9-triptycyl)ethynyl]benzene (**2**), which had been shown to crystallize in the desired manner but with the inclusion of bromobenzene. Using crystals of **2** with a ^{2}H-labeled phenylene rotator, we determined by quadrupolar echo ^{2}H NMR line shape analysis that rotation occurs by a 180° site exchange (2-fold flip) with frequencies in the MHz regime at low temperatures (150−183 K). From the temperature dependence of the rotational exchange frequency, we determined a barrier of 4.4 kcal/mol, which is only 1.4 kcal/mol higher than the internal barrier for ethane in the gas phase. Additional spectral narrowing observed at higher temperature was analyzed in terms of a model that considers larger amplitude excursions between the 180° jumps.

Introduction

Recognizing that macroscopic and biological machines are dense assemblies of moving parts in well-defined and relatively static frames of reference, we suggested that crystalline solids should offer some advantages for the development of artificial molecular machinery.[1] The premise of our work rests on the assumption that one may identify, synthesize, and refine structural motifs with degrees of freedom that involve controllable internal motions, and that the corresponding crystal structures may be rendered functional with the proper spectroscopic, dielectric, or magnetic attributes.[1,2] Alternatives based on phase transitions[3] and the use of molecules attached to various types of surfaces[4] have also been suggested and explored. To describe the coexistence of highly mobile and rigid elements within an ordered crystalline array, we suggested the term "amphidynamic crystals",[1] and we proposed structural designs based on (a) free volume compartments, (b) volume-conserving motions, such as the rotation of a cylinder along its principal axis, and/or (c) the concerted motion of two or more components.

Our initial efforts toward the design and preparation of amphidynamic crystals have centered on molecular rotors[5] that emulate the structure of macroscopic gyroscopes, either as molecular aggregates[6−8] (Figure 1) or in extended metal−organic frameworks (MOFs).[9] As illustrated in Figure 1, a simple but promising structural motif that we have recently explored with some success[6−8] consists of a central phenylene rotator linked by a nearly barrierless[10] diacetylene axle (shown in red) to a stator that consists of two bulky triptycyl[6,7] or triarylmethyl (trityl)[8] groups (shown in blue). While the stator in Figure 1 has an open topology that may expose the rotator to close packing interactions with neighboring molecules, it is known that bulky substituents at the ends of a rigid rod (wheel and axle structures)[11] lead to poor surface complementarities, low crystal densities, solvent incorporation, and perhaps faster rotational motion.[12]

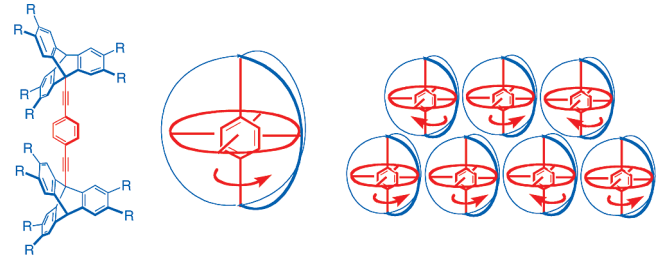

Figure 1. Suggested structural analogies between a molecular and a toy gyroscope, and an illustration of a crystalline array with units experiencing independent (Brownian) rotational motion despite being part of a close packed array.

We have recently shown that structures prepared with trityl groups display solid-state rotational dynamics that depend on the steric bulk of the substituents, with NMR-determined barriers that range between 6−8 kcal/mol.[8,12] Hoping to take advantage of the more rigid tryptycene stators to engineer lower rotational barriers, we explored the possibility of controlling the packing environment around the rotator by refining the structure of the molecular components, as illustrated by the transformation shown in Figure 2.[6,7] Diffraction-quality crystals of compound **1** grown from *meta*-xylene were characterized by a tightly interdigitated packing arrangement. As the protruding triptycenes of one molecule fill the voids left by the central phenylene of its neighbors in order to exploit favorable face-to-face and face-to-edge interactions, they prevent the rotary motion of the latter in the crystal. As indicated in the left frame of Figure 2b, the solvent molecules fill the voids formed when neighboring molecules interdigitate by offsetting with respect to their principal axis. Compound **2** was designed with the expectation that the methyl substituents on the periphery of the triptycenes would prevent the interdigitation observed in crystals **1** and the propyl groups were introduced to improve the solubility of the

* To whom correspondence should be addressed. E-mail: mgg@chem.ucla.edu.

10.1021/cg801065a CCC: $40.75
Published on Web 04/30/2009

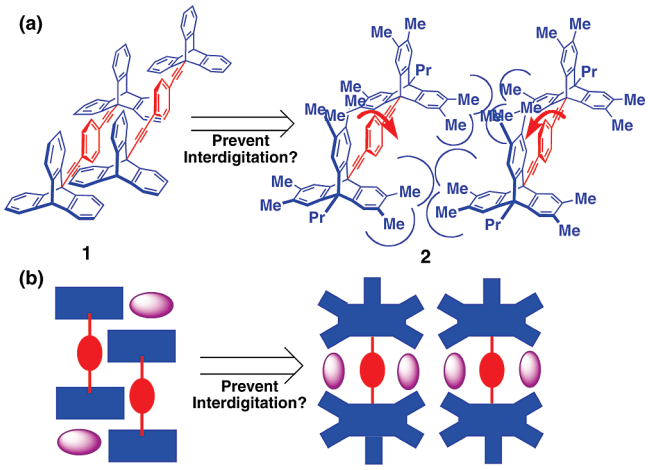

Figure 2. (a) Line formulas of **1** and **2** with representations of their packing arrangements and how the methyls on the periphery of **2** help create a lower-density environment around the central phenylene. (b) A scheme of the same structures with the position of solvent molecules illustrated. The stator components are represented in blue, the rotator and axle are in red, and the solvent molecules are in purple.

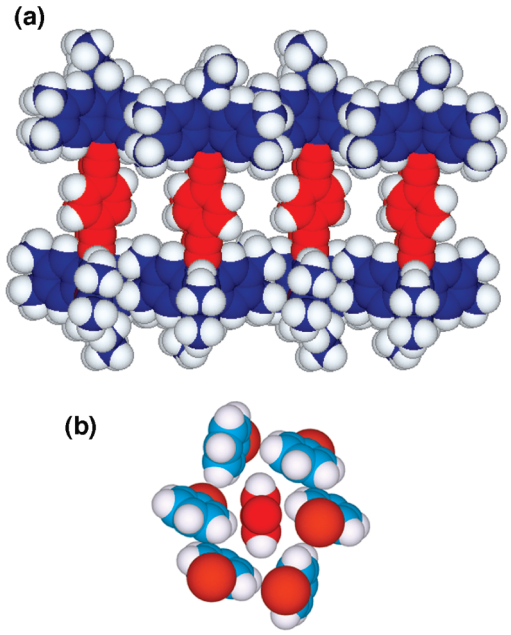

Figure 3. (a) Space-filling representation of the layer structure present in crystals of compound **2** with the solvent molecules removed. (b) Cross section down the 1,4-phenylene axis of molecular gyroscope illustrating how the rotator is surrounded by six bromobenzene molecules. The triptycene stators are shown in blue, the phenylene rotators are in red, and the bromo-benzene molecules are in light blue and orange.

sample. X-ray diffraction data of a single crystal of **2** grown from bromobenzene confirmed the expectations of our design with all the molecules oriented in the same direction to form layers segregated by the propyl groups at the two bridgehead positions (Figures 2a and 3a). The local environment around the central phenylene is shared by six bromobenzene molecules arranged in a cyclic array of parallel displaced and face-to-edge interactions (Figure 3b).

While the methyl substituents in **2** resulted in the expected changes, it was not obvious that the resulting packing structure should have more free volume than that of **1**, or that one could count on an improvement of the rotary dynamics. Fortunately,

Table 1. Selected Crystallographic Parameters, Molecular Volumes (V_{Mol}) and Packing Coefficient (C_k) of Compounds 1 and 2[a]

property	**1**	**2**
empirical formula	$C_{50}H_{30}\cdot C_8H_{10}$	$C_{68}H_{66}\cdot 2C_6H_5Br$
formula weight	736.94	1197.23
space group	$P\bar{1}$	$P\bar{1}$
Z	2	2
V, Å^3	1977.3	3231.9
ΣV_{Mol},[b] A^3	1671.6	2097.1
C_k	0.85	0.65

[a] Data for compounds **1** and **2** was taken from refs 6 and 7, respectively. [b] The volumes of the molecules in the unit cells were calculated by a group increment approach with values reported in ref 14.

a measure of the free space in crystals of **1** and **2** in terms of their packing coefficients (C_k) revealed an encouraging difference (Table 1).[13,14] With $C_k = 0.85$ and $C_k = 0.65$, respectively, crystals of **1** and **2** are at the extremes of values observed for molecular crystals.[13] We reasoned that in addition to the smaller packing coefficient of **2**, a large improvement in rotational dynamics might be aided by degrees of freedom experienced by the bromobenzene molecules in the lattice.[15] These may include small translations that change the shape of the rotator cavity and gearing motions involving rotations about their own 1,4-axis. As the first step to explore the rotary motion in crystals of **2**, we decided to analyze the rotation of the central phenylene, and as in previous studies,[8,12] by taking advantage of variable temperature quadrupolar echo ^{2}H NMR measurements with phenylene-d_4 labeled samples. The results reported here indicate a rapid site exchange between energy minima related by the expected 180° rotation in the temperature range of 150−183 K. Analysis of the temperature dependence of the exchange frequency unveiled the lowest energy barrier for rotation of a *para*-phenylene encountered so far, E_a = 4.4 kcal/mol. Additional narrowing of the spectral line width observed at higher temperatures is consistent with a rotary system that approaches continuous motion, with large angular displacements between the 180° jumps.

Experimental Section

1,4-Bis{2[(9-(10-propyl-2,3,6,7,12,13-hexamethyltriptycyl)]-ethynyl]}benzene-d_4 (2-d$_4$) was synthesized in a fashion similar to the compound with natural isotopic abundance, as reported in ref 7. Analysis: ^{1}H NMR (500 MHz, $CDCl_3$, TMS) δ 1.41 (t, J = 7.3 Hz, 6H, -($CH_2CH_2CH_3$)$_2$), 2.18 (s, 18H, Ar-CH_3), 2.19 (s, 18H, Ar-CH_3), 2.21 (m, 4H, -($CH_2CH_2CH_3$)$_2$), 2.88 (m, 4H, -($CH_2CH_2CH_3$)$_2$), 7.14 (s, 6H, Ar), 7.56 (s, 6H, Ar); ^{13}C (126 MHz, $CDCl_3$, TMS) δ 16.00, 18.60, 19.52, 19.80, 30.48, 51.69, 52.30, 87.31, 92.05, 123.38, 123.56, 131.88 (triplet, J = 24.57 Hz, -Ar-D), 132.45, 132.82, 133.01, 143.62, 143.93; ^{2}H (92 MHz, $CHCl_3$, TMS) δ 8.01 (singlet, phenylene-D).

^{2}H NMR Spectra. About 50 mg of a fine powdered sample was placed in a 5 × 32 mm glass tube and inserted in the probe of Bruker Avance instrument with a ^{2}H NMR frequency centered at 46.073 MHz using a selenoid single channel probe with a 5 mm insert. Pulse widths and phases were carefully adjusted before recording the spectra, which were acquired using the quadrupole echo pulse sequence. A 90° pulse length of 2.0 μs was used with echo and refocusing delays of 30 and 20 μs, respectively, and a delay between pulses of 60 s. Calibrated temperature determinations were carried out with a copper-constantan thermocouple carefully positioned near the sample.

^{2}H Line Shape Simulations. Spectra were fit with the program described by Nishikiori et al.[16] The input to the program consists of a model with the proper exchange positions described by the corresponding Euler angles, the site populations, and exchange rates using a quadrupolar coupling constant value e^2qQ/h = 180 kHz for the aromatic deuterons. The asymmetry parameter (η) was assumed to be 0 in all cases, and exchange rates between 10^4 and 10^7 s^{-1} were obtained by visual comparison of the experimental and simulated spectra using a line broadening of 3 kHz. While spectra measured between 150 and

Scheme 1

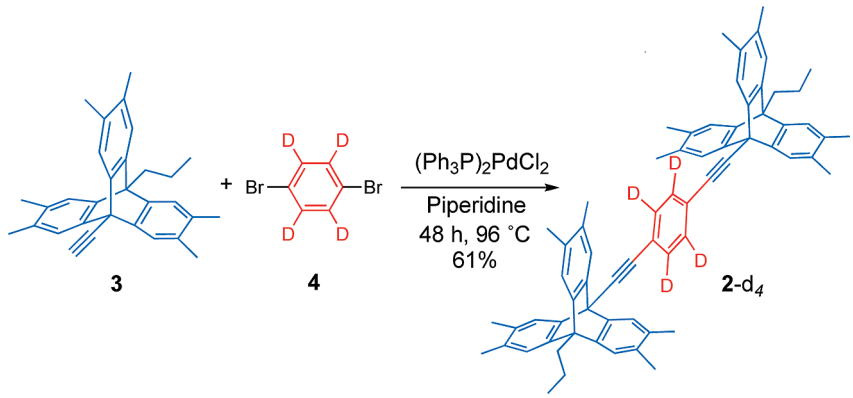

183 K could be simulated well by a 2-fold flip model, spectra acquired at higher temperature required simulations with additional an additional narrowing mechanism.

Results and Discussion

Sample Preparation. Compound **2**-d_4 was prepared as previously described for the natural abundance sample using 2 equiv of 10-propyl-2,3,6,7,12,13-hexamethyl-9-ethynyl triptycene (**3**) per equivalent of 1,4-dibromobenzene-d_4 (**4**) (Scheme 1).[7] The identity of **2**-d_4 was confirmed by NMR measurements in $CDCl_3$. As expected, a signal corresponding to the central phenylene at 7.96 ppm in the ^{1}H NMR was absent. A weak signal at 131.88 ppm in the ^{13}C NMR showed the expected hyperfine coupling (triplet, $J_{CD} = 24.6$ Hz), and a high-resolution ^{2}H NMR spectrum showed the corresponding singlet at 8.01 ppm. Samples of **2** and **2**-d_4 were crystallized from bromobenzene and shown to form identical solvent clathrates with two molecules of bromobenzene per molecular gyroscope.

Phenylene Rotation. It should be noted that rotational dynamics under equilibrium conditions are determined by the thermal energy of the crystal and the details of the rotational energy surfaces (Figure 4).[1,10] Key to our structural design is the fact that the intrinsic electronic barrier for rotation about sp−sp^n sigma bonds ($n = 2, 3$) is smaller than thermal energies at ambient temperature ($k_BT = 0.592$ kcal/mol at 300 K).[10] Under those conditions, the barrier for rotation in the solid state is governed by steric contacts with close neighbors, suggesting that properly designed crystal structures may approach the limit of continuous motion (ca. 10^{12} s^{-1}).[17] Assuming a simple 2-fold sinusoidal potential function, for thermal energies well below E_a the motion of the phenylene group can be ideally described as a harmonic oscillator with Boltzmann averaged oscillatory amplitudes and frequencies that depend on the height of the barrier (E_a) and the temperature (T). Rotation in this case occurs as discrete (Brownian) jumps between adjacent energy minima with 180° displacements determined by the symmetry of the potential.[18] In the case of hindered phenylenes, jumps occur with equal probability in either direction (clockwise or counterclockwise) in a process also known as a "two-fold flip" (Figure 4).[19] For thermal energies that are well-above E_a, the system may be described as a free rotor with degenerate states ($\pm J_n$) that describe continuous inertial rotation in either direction.

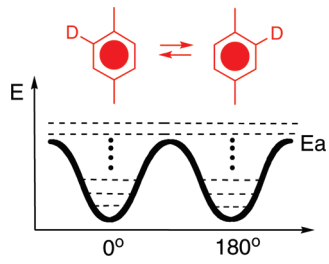

Figure 4. Idealized rotational potential of the central phenylene indicating the two energy minima separated by 180° angular displacements.

Solid-State ^{2}H NMR. It is well-known that ^{2}H NMR is one of the most powerful methods to determine internal molecular dynamics in the solid state.[20] Deuterium NMR is largely dominated by the orientation-dependent interaction between the nuclear spin and electric quadrupole moment at the nucleus. The broad spectrum from molecules in static powdered samples, also known as a Pake, or powder pattern, is strongly affected by internal molecular motions (Figure 5). Changes in the spectra occur when the C−^{2}H bonds experience reorientations that reduce their magnetic interactions by dynamic averaging.[21] For a given process, the dynamic range covered by the intermediate exchange regime includes about 4 orders of magnitude, ca. $10^3 < k_R < 10^7$ s^{-1}. Changes in line shape depend on the types of motion and their characteristic exchange frequencies.

The simulated spectra for a sample with phenylene groups having a quadrupolar coupling constant QCC = 180 kHz undergoing 2-fold flips are illustrated in Figure 5.[20,22] For an ideal crystal with a low rotational barrier, the spectrum obtained at very low temperatures should have a line shape characteristic of the slow exchange regime ($k_{180°} < 10^4$ s^{-1}, Figure 5a). The simulated spectrum from samples with phenylene groups undergoing a fast 180° exchange is illustrated in Figure 5b ($k_{180°}$

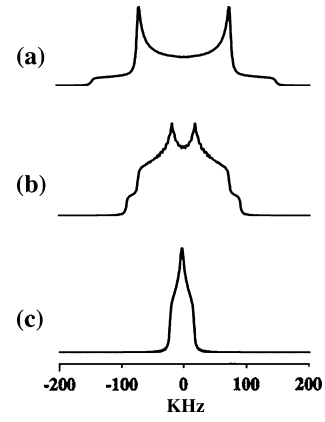

Figure 5. Quadrupolar echo ^{2}H NMR spectra for phenylene groups (a) in a static polycrystalline powder sample, (b) in the fast exchange regime of a 2-fold flipping potential, and (c) a sample with continuous rotation.

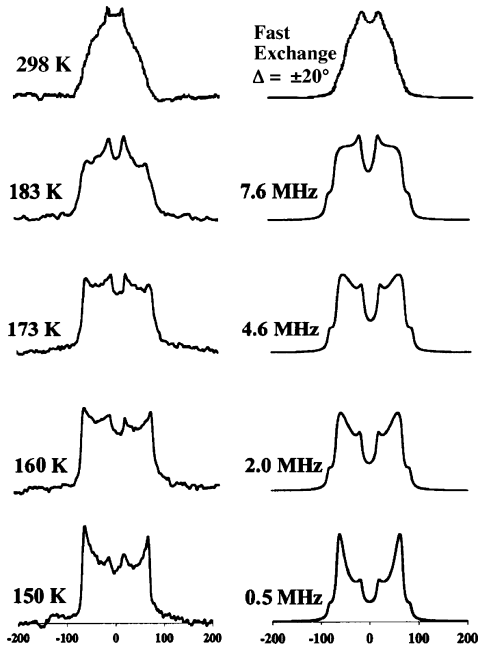

Figure 6. Experimental (left) and simulated (right) ^{2}H NMR spectra of polycrystalline **2**. Please see text for details.

$> 10^7$ s^{-1}), and one involving fast continuous rotation ($k_{Cont} > 10^7$ s^{-1}) in Figure 5c. For a sample that has no phase transitions as a function of increasing temperature, one should expect the spectrum to change in a predictable manner from the slow exchange limit into that of the fast exchange regime of the 2-fold flipping model, but further heating should narrow it further into the one characteristic of continuous rotation. The spectrum in Figure 5c would be characteristic of a crystal with a rotary process akin to that of a macroscopic gyroscope, with continuous rotation rather than discrete jumping motions.

As the ^{2}H label only represents 0.04% of the total mass in the sample, at least ca. 1500 transients had to be averaged to obtain reasonable spectra. Experiments carried at ambient temperature revealed a spectrum (Figure 6, top left) that is too narrow to fit a discrete 2-fold flipping model in the fast exchange regime (Figure 5b), and too broad to match the one expected for continuous rotation (Figure 5c). Spectra characteristic of the intermediate exchange regime were obtained between 150−183 K (Figure 6). Simulations with a 2-fold flipping model, a QCC of 180 kHz and an asymmetry parameter $\eta = 0$ gave a reasonable match with exchange frequencies of 0.5×10^6 s^{-1}, 2.0×10^6 s^{-1}, 4.6×10^6 s^{-1}, and 7.6×10^6 s^{-1} for data acquired at 150, 160, 173, and 183 K, respectively. Spectral measurements at higher temperatures (not shown) deviated from the 2-fold flipping model toward the spectrum obtained at 298 K. An Arrhenius plot (Figure 8) built with the rate and temperature data in the temperature range of 150−183 K gave an activation energy of 4.4 kcal/mol and a pre-exponential factor of 1.6×10^{12} s^{-1}, which is consistent with others reported in the literature.[8,18] It is noteworthy that the calculated activation energy is only ca. 1.4 kcal/mol higher than that for rotation of the two methyl groups of ethane in the gas phase,[23] and about seven times greater than thermal energy at 300 K.

Deviations from a 2-fold flipping model above 183 K suggest additional dynamic processes. The narrowing line shapes may be indicative of larger oscillatory amplitudes between the high frequency jumps, or a process that involves more exchange sites than the original two. Given that the environment of the rotator in the crystal structure conforms to the local 2-fold symmetry,

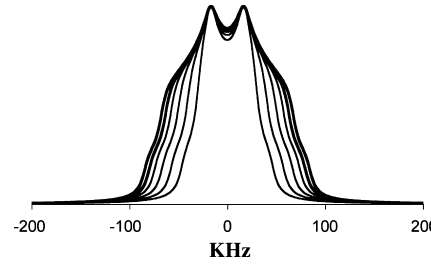

Figure 7. Spectral simulations for phenylene 180° rotations in the fast exchange regime with oscillatory amplitudes (from the outer to inner spectra) for $\pm\Delta = 0 \approx 5°$, 10°, 15°, 20°, 25°, and 30°. The width of the ambient temperature spectrum of **2** approaches the one simulated with $\Delta = 20°$.

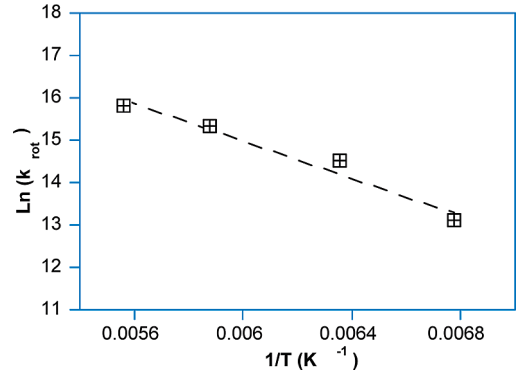

Figure 8. Arrhenius plot for the phenylene-d_4 180° site exchange derived from the variable temperature quadrupolar echo ^{2}H NMR measurements. The corresponding activation energy and pre-exponential factor are 4.4 kcal/mol and 1.6×10^{12} s^{-1}, respectively ($R^2 = 0.97$).

an exchange process involving more than two sites related by 180° would require a phase transition or a complex trajectory involving the correlated reorientation of the surrounding bromobenzene guests. To explore the role of oscillations with larger angular displacements $\Delta(^o)$ about the energy minimum, simulations were carried out by considering a fast exchange model ($k_R > 10^8$ s^{-1}) with four sites at $0° \pm \Delta°$ and $180 \pm \Delta°$, with Δ values varying between 5° and 30° (Figure 7).[24] While the result of simulations for $\Delta < 10°$ are practically indistinguishable from the normal 2-fold flipping model, excursions with $\Delta = 20$ showed a very reasonable agreement with the experimental ambient temperature spectrum (Figure 6, top).

Conclusions

In conclusion, taking the rotationally static structure **1** as the starting point, the modifications implemented in molecular gyroscope **2** met our expectations. A relatively simple change on the periphery of the triptycene groups had a profound effect on the packing arrangement and the rotational motion of the central phenylene. Remarkably, a ^{2}H NMR-determined barrier of 4.4 kcal/mol in crystals of **2** is only 1.4 kcal/mol higher than the barrier for the internal rotation of ethane in the gas phase. Studies to obtain a more complete description of molecular motion in these crystals include the preparation of samples with natural abundance **2** and bromobenzene-d_5 for line shape analysis of the latter by ^{2}H NMR, and a detailed analysis of the anisotropic displacement parameters (ADP) obtained by single crystal X-ray diffraction as a function of temperature. We believe that a methyl-substituted triptycyl stator such as that of compound **2** combined with a suitable high symmetry rotator[18]

may lead to crystals with rotational dynamics that approach the rates observed in the gas phase.

Acknowledgment. The National Science Foundation supported this work through Grant DMR-0605688.

References

(1) (a) Garcia-Garibay, M. A. *Proc. Nat. Acad. Sci. U. S. A.* **2005**, *102*, 10771–10776. (b) Khuong, T. A. V.; Nunez, J. E.; Godinez, C. E.; Garcia-Garibay, M. A. *Acc. Chem. Res.* **2006**, *39*, 413–422.

(2) Garcia-Garibay, M. A. *Angew Chem. Int. Ed.* **2007**, *46*, 8945–8947.

(3) Sokolov, A. N.; Swenson, D. C.; MacGillivray, L. R. *Proc. Nat. Acad. Sci. U. S. A.* **2008**, *105*, 1794–1797.

(4) (a) Horinek, D.; Michl, J. *Proc. Nat. Acad. Sci. U. S. A.* **2005**, *102*, 14175–14180. (b) Vacek, J.; Michl, J. *Adv. Funct. Mater.* **2007**, *17*, 730–739. (c) Zheng, X.; Mulcahy, M. E.; Horinek, D.; Galeotti, F.; Magnera, T.; Michl, J. *J. Am. Chem. Soc.* **2004**, *126*, 4540–4542. (d) Balzani, V.; Credi, A.; Venturi, M. *ChemPhysChem* **2008**, *9*, 202–220. Shirai, Y.; Morin, J. F.; Sasaki, T.; Guerrero, J. M.; Tour, J. M. *Chem. Soc. Rev.* **2006**, *35*, 1043–1055. (e) Shirai, Y.; Osgood, A. J.; Zhao, Y.; Yao, Y.; Saudan, L.; Yang, H.; Yu-Hung, C.; Alemany, L. B.; Sasaki, T.; Morin, J. F.; Guerrero, J. M.; Kelly, K. F.; Tour, J. M. *J. Am. Chem. Soc.* **2006**, *128*, 4854–4864. (f) Sasaki, T.; Osgood, A. J.; Alemany, L. B.; Kelly, K. F.; Tour, J. M. *Org. Lett.* **2008**, *10*, 229–232. (g) Nguyen, T. D.; Liu, Y.; Saha, S.; Leung, K. C. F.; Stoddart, J. F.; Zink, J. I. *J. Am. Chem. Soc.* **2007**, *129*, 626–634. (h) Nguyen, T. D.; Leung, K. C.-F.; Liong, M.; Liu, Y.; Stoddart, J. F.; Zink, J. I. *Adv. Funct. Mater.* **2007**, *17*, 2101–2110. (i) Aprahamian, I.; Yasuda, T.; Ikeda, T.; Saha, S.; Dichtel, W. R.; Isoda, K.; Kato, T.; Stoddart, J. F. *Angew. Chem., Int. Ed.* **2007**, *119*, 4759–4763. (j) Liu, Y.; Flood, A. H.; Bonvallet, P. A.; Vignon, S. A.; Northrop, B.; Tseng, H.-R.; Jeppesen, J.; Huang, T. J.; Brough, B.; Baller, M.; Magonov, S.; Solares, S.; Goddard III, W. A.; Ho, C.-M.; Stoddart, J. F. *J. Am. Chem. Soc.* **2005**, *127*, 9745–9759. (k) Nguyen, T.; Tseng, H.-R.; Celestre, P. C.; Flood, A. H.; Liu, Y.; Zink, J. I.; Stoddart, J. F. *Proc. Natl. Acad. Sci. U.S.A.* **2005**, *102*, 10029–10034.

(5) For a review of molecular rotors and the notation used to describe their components please see: Kottas, G. S.; Clarke, L. I.; Horinek, D.; Michl, J. Artificial Molecular Rotors. *Chem. Rev.* **2005**, *105*, 1281–1376.

(6) Godinez, C. E.; Zepeda, G.; Garcia-Garibay, M. A. *J. Am. Chem. Soc.* **2002**, *124*, 4701–4707.

(7) Godinez, C. E.; Zepeda, G.; Mortko, C. J.; Dang, H.; Garcia-Garibay, M. A. *J. Org. Chem.* **2004**, *69*, 1652–1662.

(8) (a) Dominguez, Z.; Dang, H.; Strouse, M. J.; Garcia-Garibay, M. A. *J. Am. Chem. Soc.* **2002**, *124*, 2398–2399. (b) Dominguez, Z.; Dang, H.; Strouse, J. M.; Garcia-Garibay, M. A. *J. Am. Chem. Soc.* **2002**, *124*, 7719–7727. (c) Khuong, T. A. V.; Zepeda, G.; Ruiz, R.; Kahn, S. I.; Garcia-Garibay, M. A. *Cryst. Growth Des.* **2004**, *4*, 15–18. (d) Khuong, T.-A. V.; Dang, H.; Jarowski, P. D.; Maverick, E. F.; Garcia-Garibay, M. A. *J. Am. Chem. Soc.* **2007**, *129*, 839–845.

(9) (a) Gould, S. L.; Tranchemontagne, D.; Yaghi, O. M.; Garcia-Garibay, M. A. *J. Am. Chem. Soc.* **2008**, *130*, 3246–3247. (b) Winston, E. B.; Lowell, P. J.; Vacek, J.; Chocholousova, J.; Michl, J.; Price, J. C. *Phys. Chem. Chem. Phys.* **2008**, *10*, 5188–5191.

(10) (a) Saebo, S.; Almolof, J.; Boggs, J. E.; Stark, J. G. *J. Mol. Struct. (Theochem)* **1989**, *200*, 361–373. (b) Sipachev, V. A.; Khaikin, L. S.; Grikina, O. E.; Nikitin, V. S.; Traettberg, M. *J. Mol. Struct.* **2000**, *523*, 1–22.

(11) (a) Toda, F.; Akagi, K. *Tetrahedron Lett.* **1968**, *9*, 3695–3698. (b) Toda, F.; Ward, D. L.; Hart, H. *Tetrahedron Lett.* **1981**, *22*, 3865–3868. (c) Hart, H.; Lin, L. T. W.; Ward, D. L. *J. Am. Chem. Soc.* **1984**, *106*, 4043–4045.

(12) Gould, S. L.; Rodriguez, R. B.; Garcia-Garibay, M A. *Tetrahedron* **2008**, *64*, 8336–8345.

(13) The packing coefficient is defined as the ratio of the volume of the molecules in the unit cell to the volume of the unit cell, $C_k = V_{mol}/V_{cell}$: Kitaigorodsky, A. I. *Molecular Crystals and Molecules*; Academic Press: New York, 1973.

(14) Gavezzotti, A. Molecular volumes were calculated with a group increment approach using the values reported by Gavezzotti. *J. Am. Chem. Soc.* **1990**, *105*, 5220–5225.

(15) Jarowski, P. D.; Houk, K. N.; Garcia-Garibay, M. A. *J. Am. Chem. Soc.* **2007**, *129*, 3110–3117.

(16) Nishikiori, S.; Soma, T.; Iwamoto, T. *J. Incl. Phenom.* **1997**, *27*, 233–243.

(17) The rotational frequency for a free rotor was calculated using a principal moment of inertia along the phenylene 1,4-axis of 80.1 g/mol Å^2 (calculated with CS Chem3D Prom CambridgeSoft) as described in Kawski, A. *Crit. Rev. Anal. Chem.* **1993** *23*, 459−529.

(18) Karlen, S. D.; Ortiz, R.; Chapman, O. L.; Garcia-Garibay, M. A. *J. Am. Chem. Soc.* **2005**, *127*, 6554–6555.

(19) (a) Cholli, A. L.; Dumais, J. J.; Engel, A. K.; Jelinski, L. W. *Macromolcules* **1984**, *17*, 2399–2404. (b) Rice, D. M.; Witebort, R. J.; Griffin, R. G.; Meirovich, E.; Stimson, E. R.; Meinwald, Y. C.; Freed, J. H.; Scheraga, H. A. *J. Am. Chem. Soc.* **1981**, *103*, 7707. (c) Rice, D. M.; Meinwald, Y. C.; Scheraga, H. A.; Griffin, R. G. *J. Am. Chem. Soc.* **1987**, *109*, 1636–1640. (d) Rice, D. M.; Blume, A.; Herzfeld, J.; Wittebort, R. J.; Huang, T. H.; DasGupta, S. K.; Griffin, R. G. *Biomol. Stereodyn., Proc. Symp.* **1981**, *2*, 255–270.

(20) Hoatson, G. L.; Vold, R. L. *NMR Basic Princ. Prog.* **1994**, *32*, 1–67.

(21) (a) Kamihira, M.; Naito, A.; Tuzi, S.; Saito, H. *J. Phys. Chem. A* **1999**, *103*, 3356–3363. (b) Hiraoki, T.; Kogame, A.; Norio, N.; Akihiro, T. *J. Mol. Struct.* **1998**, *441*, 243–250. (c) Zhang, H.; Bryant, R. G. *Biophys. J.* **1997**, *72*, 372. (d) Naito, A.; Izuka, T.; Tuzi, S.; Price, W. S.; Hayamizu, K.; Saito, H. *J. Mol. Struct.* **1995**, *355*, 55–60.

(22) Mantsch, H. H.; Saito, H.; Smith, I. C. P. *Prog. NMR Spec.* **1977**, *11*, 211–272.

(23) (a) Ercolani, G. *J. Chem. Educ.* **2005**, *82*, 1703–1708. (b) Schreiner, P. R. *Angew. Chem., Int. Ed.* **2002**, *41*, 3579–3582, and references therein.

(24) (a) Aliev, A. E.; Harris, K. D. M.; Champkin, P. H. *J. Phys. Chem. B* **2005**, *109*, 23342–23350. (b) Hallock, K. J.; Lee, D. K.; Ramamoorthy, A. *J. Chem. Phys.* **2000**, *113*, 11187–11193.

CG801065A